

Article

Dynamic Modeling and Simulation of the Sulfur Combustion Furnace in Industrial Smelter

Amine Mounaam ^{1,2,*} , Ahmed Bichri ¹, Ridouane Oulhiq ³, Ahmed Souissi ¹, Mohamed Salouhi ¹, Khalid Benjelloun ¹ and Hafid Griguer ²

¹ Ecole Mohammadia d'Ingénieurs, Mohammed V University of Rabat, Rabat 10100, Morocco

² Innovation Lab for Operations, Mohammed VI University Polytechnique, Ben Guérir 43150, Morocco

³ Technology Development Cell, Mohammed VI University Polytechnique, Ben Guérir 43150, Morocco

* Correspondence: amine.mounaam@um6p.ma

Abstract: In industrial smelters, sulfuric acid is manufactured using the elemental sulfur in a series of three-unit operations: elemental sulfur oxidation, sulfur dioxide catalytic conversion, and sulfur trioxide absorption. The sulfur oxidation, which is the basic step in this process, is generally performed under a sulfur combustion furnace that ensures the production of the process gas stream, which will be the main supply stream to the other unit operations. In this paper, a dynamic model is developed based on the fundamental mass and energy balance, including the sulfur oxidation and the dynamic flow behavior aspects within the furnace. The obtained model is simulated in the Matlab/Simulink environment and data from an industrial plant were used to validate the model. The simulation results and the plant measurement comparison showed an accuracy of 96%, with a mean absolute error of 16.12 °C and a root mean square error of 23.27 °C. Afterwards, the effect of different operating conditions and disturbance parameters on the sulfur combustion furnace performance were studied. Finally, the relationship and a correlation between the temperature and sulfur dioxide molar fraction at the outlet of the furnace were investigated for industrial use.

Keywords: sulfuric acid; sulfur oxidation; combustion furnace; sulfur burner; dynamic modeling; process simulation



Citation: Mounaam, A.; Bichri, A.; Oulhiq, R.; Souissi, A.; Salouhi, M.; Benjelloun, K.; Griguer, H. Dynamic Modeling and Simulation of the Sulfur Combustion Furnace in Industrial Smelter. *Processes* **2022**, *10*, 2655. <https://doi.org/10.3390/pr10122655>

Academic Editor: Cherng-Yuan Lin

Received: 18 October 2022

Accepted: 15 November 2022

Published: 9 December 2022

Publisher's Note: MDPI stays neutral with regard to jurisdictional claims in published maps and institutional affiliations.



Copyright: © 2022 by the authors. Licensee MDPI, Basel, Switzerland. This article is an open access article distributed under the terms and conditions of the Creative Commons Attribution (CC BY) license (<https://creativecommons.org/licenses/by/4.0/>).

1. Introduction

Sulfuric acid is an oily clear and dense liquid that is considered as one of the most important chemical reactants [1]. It is involved in the phosphoric acid industry, fertilizer manufacturing, and the petroleum-refining processes. Industrial sulfuric acid production began in the 18th century with two processes, namely the lead chamber process and the tower process [2]. Unfortunately, their performance was limited in terms of the sulfuric acid strength, with a mass concentration that did not exceed 70%. Thus, they were replaced by the contact process in the 20th century, which economically produces sulfuric acid with different concentrations [3]. Note that the contact process has experienced several modifications, such as the transition from single absorption to double absorption and the integration of the heat-recovery system. Operating with double absorption instead of single makes it possible to reach a conversion rate of 99.5% and higher [4].

The contact process includes three main steps: sulfur oxidation, sulfur dioxide SO₂ catalytic conversion, and sulfur trioxide SO₃ absorption. However, sulfur oxidation is considered the most important step in the sulfuric acid production line, as all the remaining process units are based on the characteristics of the gas mixture leaving the combustion furnace [5]. Industrially, three types of sulfur combustion burners are generally used: rotary burner, acme burner, and spray-type burner [6]. In the latter, the molten sulfur is transformed into tiny droplets using stationary spray nozzles and then it is injected into the combustion chamber, in which the atomized sulfur reacts with the oxygen contained in the air combustion. The oxidation reaction of the liquid sulfur is a highly exothermic

reaction that generates a significant amount of heat. Thus, a heat-recovery boiler is placed right at the outlet of the sulfur combustion furnace, to recover a part of the combustion reaction heat and produce steam.

Considering the importance of this process, modeling and simulation techniques and optimization tools are progressively employed at both laboratory and industrial scales to fully understand and monitor the manufacturing plans in an optimal way [7,8]. Thus, many models were developed to simulate and optimize the sulfuric acid process efficiency. In [5], an industrial sulfuric acid plant was modeled and simulated using gPROMS. The model included a four-bed catalytic reactor, heat exchangers, mixers, splitters, and absorption towers. However, the paper ignores the dynamics of the sulfur burner. In [9], a simplified sulfuric acid process was simulated in steady state using Aspen HYSYS. For the model parameter's values, data from an industrial plant were used. Then, the simulation results were employed to optimize the studied process' annual profit. Likewise, Aspen One was also tested to design and simulate a sulfuric acid process [10]. However, the used models were not detailed and the results lack industrial validation. In [11], Aspen Plus was used to develop a complete model of a single-absorption sulfuric acid plant with a scrubbing tower, but the used model details were not included. Regarding the catalytic conversion of SO_2 into SO_3 , several studies were performed to model and simulate the performance of the conversion reactor. In [12], authors used a pseudo-homogeneous perfect plug flow model to describe the performance of the SO_2 catalytic converter, which was solved in the COMSOL Multiphysics environment. In [13], a SO_2 oxidation reactor was simulated using a dynamic tanks-in-series model; the obtained results were validated using experimental and industrial measurements. As well, a dynamic model based on energy and mass balance equations was established for a SO_2 conversion reactor simulation in industrial smelter. The proposed model was compared with industrial data and used to study the process' variable effects on the dynamic response of the converter [14]. Using the Unisim Design R451 simulator, an industrial SO_2 conversion unit, including a four-bed reactor and three heat exchangers, was modeled and simulated in steady state and dynamic mode [15]. After validating the developed model, the dynamic response of the catalytic conversion was widely studied and a digital twin framework was proposed to simulate the studied unit in real time. In [16], a multi-objective optimization study was carried out to maximize the SO_2 conversion rate and productivity and minimize the catalyst weight required for the catalytic conversion reaction. Thus, a compromise was highlighted between the SO_2 conversion rate, the process productivity, and the required catalyst weight.

Based on the literature review, research works on modeling and simulating the sulfuric acid process ignore the importance of the sulfur combustion furnace. In our previous work [17], the Unisim Design R451 simulator was used to simulate an industrial sulfur combustion unit. The simulation model included a liquid sulfur pump, combustion air blowers, and a simple conversion reactor for the sulfur burner modeling. However, the global model neglected the dynamic flow of the combustion gas mixture within the combustion furnace.

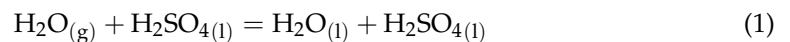
The present work aims to develop a dynamic model for the sulfur combustion reactor, so that it can be efficiently and easily deployed in an industrial smelter. Thus, a dynamic model is developed to simulate and optimize the performance of the industrial sulfur combustion furnace within sulfuric acid plants. The proposed model is developed based on the fundamental mass and energy balance equations and includes both the combustion reaction aspect and the dynamic flow behavior of the combustion gas in the combustion chamber. The proposed model is validated using comprehensive industrial data from various periods that include all the process operating points. In addition, a user-friendly graphical interface is incorporated in the developed model to make it well suited for industrial use. Finally, a parametric study is conducted to answer the what-if type questions related to the sulfur combustion furnace operation and understand the relationship between the system inlets and outlets.

This paper is organized as follows: the sulfur combustion furnace is described in Section 2. The proposed model is then detailed in Section 3. A dynamic simulation of the

developed model is performed in Section 4 and a validation step using industrial data is conducted in Section 5. Section 6 presents the parametric study results and discussion, while Section 7 concludes the paper.

2. Process Description

Industrially, sulfuric acid H_2SO_4 is generally manufactured using the double-contact process, in a series of four principal steps: combustion air drying, sulfur oxidation with oxygen O_2 , sulfur dioxide SO_2 catalytic oxidation, and finally sulfur trioxide SO_3 absorption. The three chemical reactions involved in this process are given as follows [18]:



Firstly, the wet air is dried in an absorption tower, in which the circulating H_2SO_4 absorbs the humidity contained in the wet air according to the Equation (1). After drying the air, the liquid sulfur feeds the sulfur furnace combustion and reacts with the O_2 contained in dry air in terms of the Equation (2). The liquid sulfur combustion is an exothermic reaction that produces the necessary SO_2 amount for the conversion step. Then, the gas mixture (O_2 , N_2 , SO_2) feeds the catalytic converter, in which the SO_2 reaction with the O_2 produces SO_3 following the catalytic conversion reaction (3). After a series of heat-exchanging operations, the gas mixture (O_2 , N_2 , SO_2 , SO_3) passes through an intermediate absorption unit to produce H_2SO_4 according to the reaction (4). Thereafter, the gas turns back to the conversion unit, in which the rest of SO_2 contained in the gas mixture is converted to SO_3 before feeding the final absorption tower.

Thus, sulfur furnace combustion has a major role in the manufacture of sulfuric acid in an industrial smelter. It is considered as the most important step in this production line, since the remaining process units are based on the gas mixture properties leaving the furnace. The combustion furnace (Figure 1) is a horizontal chamber with cylindrical form, made of several material layers, such as carbon steel and insulation bricks, to minimize heat-transfer losses in the surroundings [4].

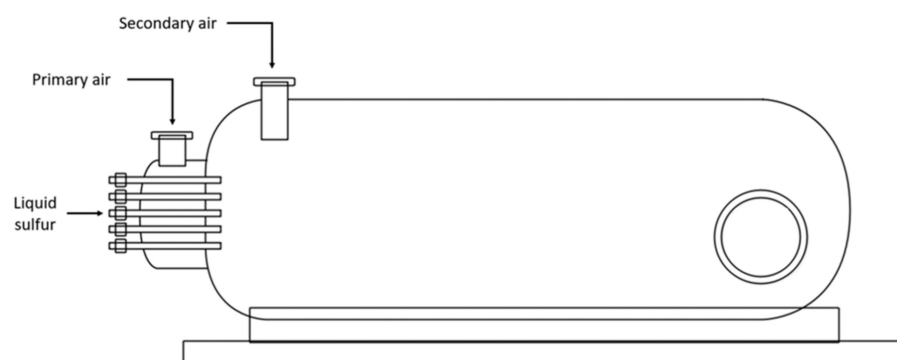


Figure 1. Industrial sulfur combustion furnace.

The molten sulfur feeds the sulfur furnace using a stationary spray nozzle or spinning-cup atomizer, at a temperature around $140\text{ }^\circ\text{C}$ that corresponds to a lower viscosity value of the liquid sulfur. Note that its viscosity can increase dramatically from $0.01\text{ kg/m}\cdot\text{s}$ to $100,000\text{ kg/m}\cdot\text{s}$, just above a temperature of $160\text{ }^\circ\text{C}$ [19]. This change in the liquid sulfur viscosity can be justified by the transition of the sulfur ring molecules to long interwoven sulfur chain molecules [20]. The vaporization of the liquid sulfur is then realized at a boiling temperature of $445\text{ }^\circ\text{C}$ in the hot furnace due to the tiny droplets produced by the

sulfur atomizer. The tiny and warm droplets of the molten sulfur make it possible to ensure its rapid vaporization and fast and complete oxidation within the hot furnace. The dry air used for the sulfur combustion feeds the sulfur furnace using air blowers and in behind the liquid sulfur spray to increase the contact between the sulfur droplet and the air. The air is injected into the combustion chamber from two positions: the primary air supply that feeds the sulfur furnace from its principal entry and the secondary one that feeds the combustion chamber to ensure a higher gas turbulence and a complete oxidation of the atomized sulfur. The gas mixture leaves the sulfur furnace with a chemical composition at a temperature of 1150 °C and a chemical component composition of 12%, 9%, and 79% of SO₂, O₂, and N₂, respectively [19].

3. Sulfur Combustion Furnace Model Development

For the sulfur combustion furnace model development, the following assumptions were considered: (1) the liquid sulfur droplets are tiny and are rapidly vaporized, (2) the gas mixture is homogeneous and incompressible, (3) the gas flow is one-dimensional in the axial direction Z, (4) the gas is radially isotropic, and (5) the pressure drop and the heat transfer via radiation are neglected.

In chemical process design and modeling, reactor equation models are not developed according to their external form, but on describing the phenomena involved in the reactor [21]. However, reactor sizes and material properties are also taken into consideration while establishing the model equations. Thus, each reactor model can be elaborated based on the fundamental mass, energy, and momentum balance equations, instead of the kinetic description of the chemical reactions in case there are any that govern the reactor operation.

3.1. Mass Balance Equation

The mass balance equation is used to describe the variation in the component's concentration within the reactor according to the inlets, outlets, component consumption or production, and the accumulation within the studied reactor. The most common mathematical form used to describe the mass conservation equation in chemical processes is given as follows [22]:

$$\frac{\partial C_i}{\partial t} + \nabla(C_i \cdot U) + \nabla \cdot J_i = R_i \quad (5)$$

where:

- C_i: component «i» molar concentration (mol/m³);
- U: average velocity (m/s);
- J_i: molar diffusivity flux (mol/m².s);
- R_i: component «i» rate change (mol/m³.s).

The first term in the mass balance equation from the left side presents the component «i» accumulation, the second term describes the component transport by convection, while the third term describes the component transport by diffusion. When it comes to the right-side term of the mass balance equation, it represents the component rate change caused by consumption or production of the component in case of one or multiple chemical reactions.

By dividing the equation above by the molecular-weight M_i (g/mol) of the component «i» and applying it over all the gas components, the following is obtained:

$$\sum_i \frac{\partial C_i \cdot M_i}{\partial t} + \sum_i \nabla(C_i \cdot M_i \cdot U) + \sum_i M_i \cdot J_i = \sum_i M_i \cdot R_i \quad (6)$$

The gas density ρ (kg/m³) can be computed according to component concentration and molecular weight M_i (kg/kmole) as:

$$\rho = \sum_i C_i \cdot M_i \quad (7)$$

Thus, Equation (6) can be written in terms of the gas density by:

$$\frac{\partial \rho}{\partial t} + \nabla(\rho \cdot U) + \sum_i M_i \cdot J_i = \sum_i M_i \cdot R_i \quad (8)$$

Regarding the definition of mass conservation within a reaction system, the terms $\sum_i M_i \cdot J_i$ and $\sum_i M_i \cdot R_i$ are equal to zero. Thus, the total continuity equation can also be achieved:

$$\frac{\partial \rho}{\partial t} + \nabla(\rho \cdot U) = 0 \quad (9)$$

Under assumption (3), the total continuity equation and the mass balance equation can be simplified:

$$\begin{cases} \frac{\partial C_i}{\partial t} + \nabla(C_i \cdot U) + \nabla \cdot J_i = \frac{\partial C_i}{\partial t} + U \cdot \nabla C_i + \nabla \cdot J_i = R_i \\ \frac{\partial \rho}{\partial t} + \nabla(\rho \cdot U) = \rho \cdot \nabla(U) = 0 \end{cases} \quad (10)$$

The molar flux vector J_i in the component «i» can be expressed based on the diffusion Fick law [23], in terms of its binary diffusivity $D_{i,f}$ (m^2/s):

$$J_i = \rho \cdot D_{i,f} \cdot \nabla \frac{C_i}{\rho} \quad (11)$$

In cylindrical coordinates and under assumptions (3) and (4), we obtain the following species mass balance equation:

$$\frac{\partial C_i}{\partial t} + U^z \cdot \frac{\partial C_i}{\partial z} + D_{i,f}^z \cdot \frac{\partial^2 C_i}{\partial z^2} = R_i \quad (12)$$

Note that the molecular diffusion aspect is usually neglected while performing with a highly turbulent flow. Thus, the species mass balance equation can be more simplified as follows:

$$\frac{\partial C_i^z}{\partial t} + U^z \cdot \frac{\partial C_i^z}{\partial z} = R_i \quad (13)$$

The obtained species mass balance equation can take another preferable form, in terms of component molar fraction X_i , which is widely used in chemical reactor study. A component molar fraction X_i can be expressed in function of its molar concentration C_i as:

$$X_i = C_i \frac{M}{\rho} \quad (14)$$

3.2. Energy Balance Equation

The energy balance equation, or the enthalpy balance equation, is used to describe the heat-exchange phenomena involved in the system. By similarity to the mass balance equation, the energy balance equation can also be obtained according to the system inlet and outlet enthalpy, heat consumption or generation due to chemical reactions, and the heat accumulation within the system. Note that chemical process potential as well as kinetic and work energies are generally neglected. In a rectangular coordinate system, the popular form of the energy balance equation used in reactor design and modeling is given by [22]:

$$\frac{\partial H}{\partial t} + \nabla(H \cdot U) + H_f = H_R + H_C + H_{rad} + H_{loss} \quad (15)$$

In the above equation, the first term from the left side presents the heat accumulation within the system, the second term describes the heat conduction flow due to the convection, and the third term is the diffusion heat flow due to molecular diffusion. In the right side of the equation, the first term gives the heat generated or consumed by chemical reactions, the second term describes the conduction heat flow, the third one presents the heat flow

exchanged by radiation, which is neglected in this case, and the last one describes the heat flow loss exchanged with the reactor through the wall. Thus, by replacing each type of heat in the energy balance equation with its corresponding term, the following developed equation is obtained:

$$\rho \cdot c_p \frac{\partial T}{\partial t} + U \cdot \rho \cdot c_p \cdot \nabla(T) = \sum_i (-\Delta_{r,i} H \cdot R_i) + \nabla \cdot (\lambda \cdot \nabla T) + \frac{4 \cdot U_{\text{loss}}}{D_r} (T_s - T) \quad (16)$$

where:

- c_p : mixture heat capacity (kJ/kg.°K);
- ρ : gas density (kJ/kg.°K);
- T : gas temperature (°K);
- H_i : component «i» molar enthalpy (kJ/kmole);
- $\Delta_{r,i} H$: reaction heat according to the component «i» (kJ/kmole of i);
- λ : gas conductivity (kJ/°K.m.s);
- T_s : surrounding temperature;
- U_{loss} : overall heat-transfer coefficient (kJ/m².°K);
- D_r : reactor diameter (m).

Using the ideal gas law, the gas mixture density and heat capacity can be approximated by:

$$\begin{cases} \rho = \sum_i x_i \cdot \rho_i \\ c_p = \sum_i x_i \cdot c_{p,i} \end{cases} \quad (17)$$

In cylindrical coordinates and under assumptions (3) to (5), the following energy balance equation is obtained:

$$\rho \cdot c_p \frac{\partial T}{\partial t} + U^z \cdot \rho \cdot c_p \frac{\partial T}{\partial z} = \sum_i (-\Delta_{r,i} H \cdot R_i) + \frac{\partial}{\partial z} \left(\lambda^z \cdot \frac{\partial T^z}{\partial z} \right) - \frac{4 \cdot U_{\text{loss}}}{D_r} (T - T_s) \quad (18)$$

3.3. Model Development

In this part, a dynamic model for the sulfur combustion furnace is developed based on the mass balance and energy balance equations. The furnace is considered as a distributed parameter system since the system variables (C_i , T) vary in time and space within the reactor, which implies that the system model equation would be described based on a partial differential equation. However, to make the model suitable for industrial uses, a reactor scheme model for the studied sulfur combustion furnace was proposed by dividing the combustion chamber into several zones, as shown in Figure 2.

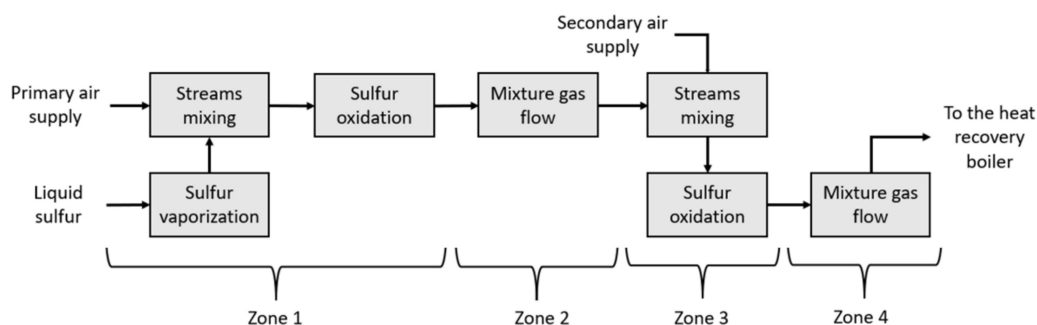


Figure 2. Reactor scheme model proposed for modeling the studied sulfur combustion furnace.

The four zones used to describe the operation of the sulfur combustion furnace are as follows: zone 1 stands for the liquid sulfur vaporization, the vaporized sulfur and the first combustion air streams mixing, and finally the atomized sulfur oxidation; zone 2 stands for the combustion mixture gas flow; zone 3 stands for the secondary air supply and maintaining sulfur oxidation; zone 4 stands for the mixture gas flow through the rest

of the furnace. From the proposed schema model, two principal subsystems can be derived: the first and third zones in which the rapid oxidation reaction of the atomized reaction takes place and the second and fourth zones in which the combustion gas mixture flows without chemical reaction.

For the atomized sulfur oxidation modeling, the liquid sulfur droplets are vaporized the first time and mixed with the primary blown air. The inlet flows are supposed to be immediately mixed with the region-remaining contents and then the oxidation reaction is produced. Note that the vaporization of the liquid sulfur is considered only in the first region of the combustion chamber. Thus, a Continuous Stirred-Tank Reactor (CSTR) model in steady state is used. The mass and energy mass balance equations can be integrated over this region volume as follows:

$$\begin{cases} \int_{Z_1^{\text{in}}}^{Z_1^{\text{out}}} U^z \frac{\partial C_i}{\partial z} dz = \int_{Z_1^{\text{in}}}^{Z_1^{\text{out}}} R_i dz \\ \int_{Z_1^{\text{in}}}^{Z_1^{\text{out}}} U^z \cdot \sum_i \rho \cdot c_p \frac{\partial T}{\partial z} dz = \int_{Z_1^{\text{in}}}^{Z_1^{\text{out}}} \sum_i (-\Delta_{r,i} H \cdot R_i) dz \end{cases} \quad (19)$$

Multiplying both sides of the system equations above by the furnace section area $A_s(\text{m}^2)$ and applying the obtained mass balance equation on the furnace inlet components:

$$\begin{cases} \dot{F}_{\text{O}_2, \text{out}} - \dot{F}_{\text{O}_2, \text{in}} = -\xi \cdot \dot{F}_{\text{S}, \text{in}} \\ \dot{F}_{\text{S}, \text{out}} - \dot{F}_{\text{S}, \text{in}} = -\xi \cdot \dot{F}_{\text{S}, \text{in}} \\ \dot{F}_{\text{SO}_2, \text{out}} = \xi \cdot \dot{F}_{\text{S}, \text{in}} \\ \dot{F}_{\text{N}_2, \text{out}} - \dot{F}_{\text{N}_2, \text{in}} = 0 \\ \dot{F}_{\text{total}, \text{out}} - \dot{F}_{\text{total}, \text{in}} = -\xi \cdot \dot{F}_{\text{S}, \text{in}} \\ \dot{H}_{\text{out}} - \dot{H}_{\text{in}} = \xi \cdot \dot{F}_{\text{S}, \text{in}} \cdot \Delta_r H \end{cases} \quad (20)$$

where:

- $\dot{F}_{i, \text{in}}$: component «i» inlet molar flowrate (mol/h);
- $\dot{F}_{i, \text{out}}$: component «i» inlet molar flowrate (mol/h);
- $\dot{F}_{\text{total}, \text{out}}$: gas mixture molar flux at the outlet (mol/h);
- $\dot{F}_{\text{total}, \text{in}}$: gas mixture molar flux at the inlet (mol/h);
- ξ : sulfur combustion reaction rate (%);
- $\Delta_r H$: combined vaporization and combustion reactions heat ($\simeq 300$ MJ/kg mol of S(l));
- $\dot{H}_{\text{T}, \text{in}}$: inlet heat flow (kJ/h);
- $\dot{H}_{\text{T}, \text{out}}$: outlet heat flow (kJ/h).

The sulfur combustion reaction rate ξ presents the amount of the atomized sulfur that was completely oxidized into SO_2 :

$$\xi = \frac{\dot{F}_{\text{S}, \text{in}} - \dot{F}_{\text{S}, \text{out}}}{\dot{F}_{\text{S}, \text{in}}} = \frac{\min(\dot{F}_{\text{S}, \text{in}}; \dot{F}_{\text{O}_2, \text{in}})}{\dot{F}_{\text{S}, \text{in}}} \quad (21)$$

The inlet and outlet heat flow are computed based on the furnace inlet and outlet properties as follows:

$$\begin{cases} \dot{H}_{\text{in}} = \int_{T_0}^{T_{\text{in}}} \sum_i \dot{F}_{i, \text{in}} c_{p,i}(T) \cdot dT \\ \dot{H}_{\text{out}} = \int_{T_{\text{in}}}^{T_{\text{out}}} \sum_i \dot{F}_{i, \text{out}} c_{p,i}(T) \cdot dT \end{cases} \quad (22)$$

where:

- T_{in} : initial temperature of the gas mixture before the oxidation reaction ($^{\circ}\text{C}$);
- T_{out} : temperature of the gas mixture after the oxidation reaction ($^{\circ}\text{C}$);
- T_0 : reference temperature ($^{\circ}\text{C}$).

The temperature T_{in} of the gas mixture (S, O_2, N_2) before the oxidation reaction can also be calculated by the same approach:

$$\int_{T_0}^{T_{A,in}} \dot{F}_{O_2,in} c_{p,O_2}(T) + \dot{F}_{N_2,in} c_{p,N_2}(T) \cdot dT + \int_{T_0}^{T_{S,in}} \dot{F}_{S,in} c_{p,S}(T) \cdot dT = \int_{T_0}^{T_{in}} \sum_i \dot{F}_{i,in} c_{p,i}(T) \cdot dT \quad (23)$$

where:

- $T_{A,in}$: inlet temperature of the combustion air ($^{\circ}C$);
- $T_{S,in}$: inlet temperature of the liquid sulfur ($^{\circ}C$).

Components' specific heat capacity $c_{p,i}(T)$ can be expressed in terms of the temperature using the following second-order polynomial approximation [24]:

$$c_{p,i}(T) = a_i + b_i T + c_i T^2 \quad (24)$$

Using Equation (24) in (23):

$$\sum_i \dot{F}_{i,out} \left[a_i T + \frac{b_i}{2} T^2 + \frac{c_i}{3} T^3 \right]_{T_0}^{T_{out}} = \sum_i \dot{F}_{i,in} \left[a_i T + \frac{b_i}{2} T^2 + \frac{c_i}{3} T^3 \right]_{T_0}^{T_{in}} + \xi \cdot \dot{F}_{S,in} \cdot \Delta_r H \quad (25)$$

For the combustion gas mixture flow modeling, the gas produced by the atomized sulfur oxidation is assumed to move as a plug one-dimensionally flow. The gas flows in the combustion chamber after the rapid and complete oxidation of the atomized sulfur by the oxygen contained in the combustion air. Thus, a Plug Flow Reactor (PFR) model is used to describe the combustion gas mixture transport within the combustion chamber. Therefore, the mass and energy balance equations can be reduced to describe the transient behavior of the gas flow by the following equation system:

$$\begin{cases} \frac{\partial C_i}{\partial t} + U^z \cdot \frac{\partial C_i}{\partial z} = 0 \\ \rho \cdot c_p \cdot \frac{\partial T}{\partial t} + U^z \cdot \rho \cdot c_p \cdot \frac{\partial T}{\partial z} = -\frac{4 \cdot U_{loss}}{D_r} (T - T_s) \end{cases} \quad (26)$$

Boundary and initial conditions required to compute the equations above are:

$$z = 0, \quad C_i(t) = C_{i,in}(t), \quad T(t) = T_{in}(t) \quad (27)$$

$$t = 0, \quad z > 0, \quad C_{SO_2}^0(z) = 0, \quad T(z) = T_f \quad (28)$$

$$z = L_r, \quad \frac{\partial C_i}{\partial z} = 0, \quad \frac{\partial T}{\partial z} = 0 \quad (29)$$

where:

- T_f : initial temperature of the combustion furnace ($^{\circ}C$);
- $C_{i,in}$: component «i» initial molar concentration in the furnace ($^{\circ}C$);
- z_{max} : total length of the combustion furnace (m).

The overall heat transfer coefficient U_{loss} can be estimated using the furnace dimensions and the constituent material properties using the following equation [25]:

$$\frac{1}{U_{loss} \cdot A_{loss}} = \frac{1}{h_r \cdot A_{r,i}} + \frac{\ln\left(\frac{r_{r,o}}{r_{r,i}}\right)}{2\pi \cdot L_r \cdot (r_{r,o} - r_{r,i}) \cdot \lambda_r} + \frac{1}{h_{amb} \cdot A_{r,o}} \quad (30)$$

where:

- A_{loss} : heat-transfer areas (m^2);
- h_r : convective heat-transfer coefficient of gas mixture ($W/m^2 \cdot K$);
- $A_{r,i}$: inner areas of the combustion chamber (m^2);
- $r_{r,i}$: inner radius of the combustion chamber ($W/m^2 \cdot K$);
- $r_{r,o}$: outer radius of the combustion chamber ($W/m^2 \cdot K$);

- h_{amb} : heat-transfer coefficient of the surrounding air ($W/m^2.K$);
- $A_{r,o}$: outer areas of the combustion chamber (m^2);
- λ_r : global thermal conductivity of the furnace several material layers ($W/m^2.K$).

Regarding the convective heat-transfer coefficient of the gas mixture within the combustion chamber, it can be computed using the three dimensionless numbers: Reynolds (Re), Prandtl (Pr), and Nusselt (Nu):

$$Re = \frac{\rho \cdot U^z \cdot D_r}{\mu} \quad (31)$$

$$Pr = \frac{\mu \cdot c_p}{\lambda} \quad (32)$$

$$Nu = \frac{h \cdot D_r}{\lambda} = f(Re, Pr) \quad (33)$$

where:

- μ : dynamic viscosity of the gas mixture ($kg/m.s$);
- λ : thermal conductivity of the gas mixture ($W/m^2.K$);
- f : function depending on the flow regime.

3.4. Global Model

Based on the mass and energy balance equations, the global model of the sulfur combustion furnace is presented in Figure 3 and deduced from Equation (20), (22), and (26) as follows:

$$\dot{F}_{O_2,out} = \dot{F}_{O_2,in} - \xi \cdot \dot{F}_{S,in} \quad (34)$$

$$\dot{F}_{S,out} = (1 - \xi) \dot{F}_{S,in} \quad (35)$$

$$\dot{F}_{SO_2,out} = \xi \cdot \dot{F}_{S,in} \quad (36)$$

$$\dot{F}_{N_2,out} = \dot{F}_{N_2,in} \quad (37)$$

$$\dot{F}_{total,out} = \dot{F}_{total,in} - \xi \cdot \dot{F}_{S,in} \quad (38)$$

$$\sum_i \dot{F}_{i,out} \left[a_i T + \frac{b_i}{2} T^2 + \frac{c_i}{3} T^3 \right]_{T_0}^{T_{out}} = \sum_i \dot{F}_{i,in} \left[a_i T + \frac{b_i}{2} T^2 + \frac{c_i}{3} T^3 \right]_{T_0}^{T_{in}} + \xi \cdot \dot{F}_{S,in} \cdot \Delta_r H \quad (39)$$

$$\frac{\partial C_i}{\partial t} + U^z \cdot \frac{\partial C_i}{\partial z} = 0 \quad (40)$$

$$\rho \cdot c_p \cdot \frac{\partial T}{\partial t} + U^z \cdot \rho \cdot c_p \cdot \frac{\partial T}{\partial z} = - \frac{4 \cdot U_{loss}}{D_r} (T - T_s) \quad (41)$$

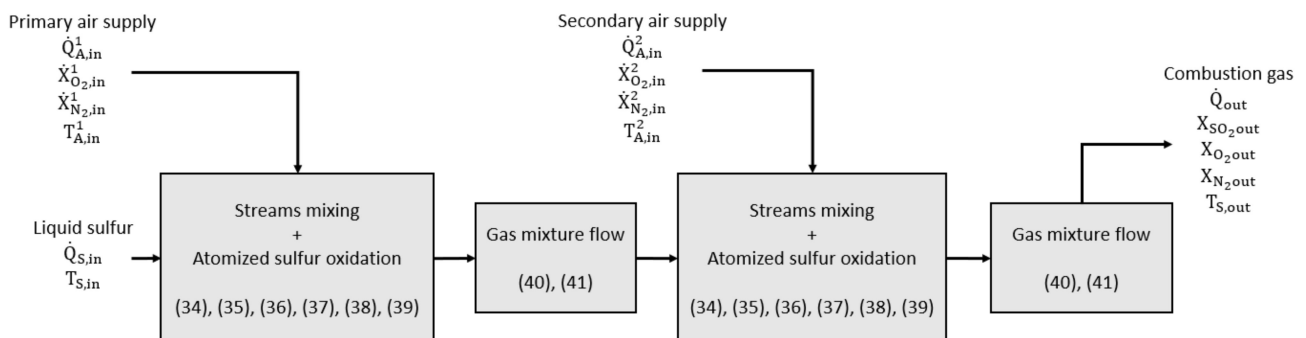


Figure 3. Sulfur combustion furnace model block diagram.

4. Model Simulation

The simulation of the studied sulfur combustion furnace was performed under a Dell Precision 5820, with Intel® Xeon® W-2123 CPU @ 3.60 GHz and a RAM of 32 Go in the environment Matlab/Simulink. Level 2 of Matlab s-functions was used to create different simulation blocks, as shown in Figure 4. S-function blocks were adopted in this study due to their capability to resolve both continuous and discrete systems [26], in addition to their flexibility and readability performance [27]. The finite-difference method was used to discretize time and space and resolve the gas-flow partial differential equation. For the axial space discretization, a first-order backward difference was applied with 100 mesh points, while a first-order forward difference was used for the time discretization, with a step size of 0.1 sec. The chosen discretization methods were used to ensure accurate stability and simplicity of the numerical computation. Table 1 summarizes the principal feed properties and initial conditions that were used to simulate the dynamic response of the studied system. The initial temperature of the furnace was set to $T_f = 900$ °C, while the gas contained in the combustion chamber was assumed to be dry air. Thus, the initial composition of the gas at the outlet of the sulfur combustion furnace was taken $C_{SO_2}^0 = 0$, $C_{O_2}^0 = 21\%$ and $C_{N_2}^0 = 79\%$.

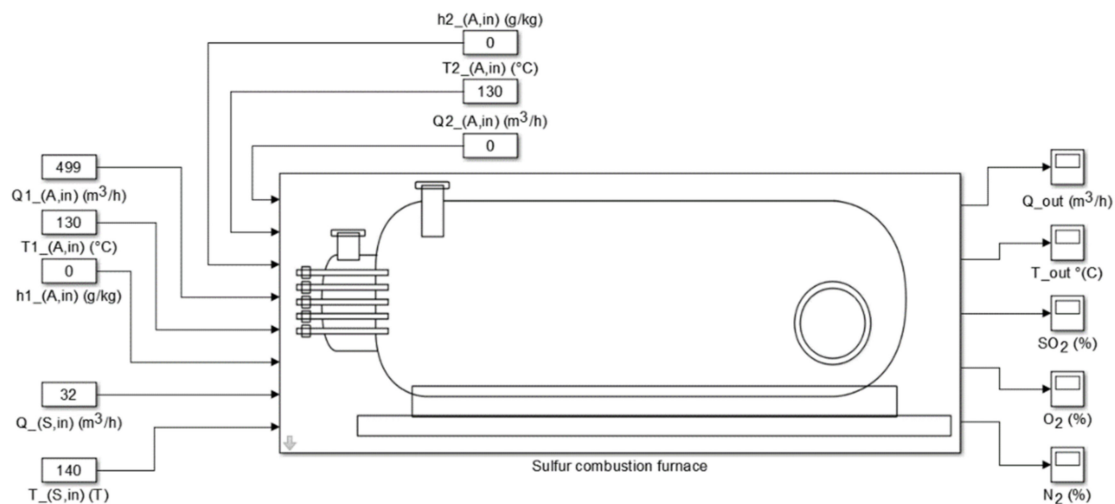


Figure 4. Sulfur combustion furnace simulation using Matlab/Simulink.

Table 1. Simulation parameters.

Parameters	Description	Value	Unit
$\dot{Q}_{A,in}^1$	Primary air flowrate	499	m ³ /h
$T_{A,in}^1$	Primary air temperature	130	°C
$h_{A,in}^1$	Primary air relative humidity	0	g/kg
$\dot{Q}_{S,in}$	Liquid sulfur flowrate	32	m ³ /h
$T_{S,in}$	Liquid sulfur temperature	132	°C
$\dot{Q}_{A,in}^2$	Secondary air flowrate	0	m ³ /h
$T_{A,in}^2$	Secondary air temperature	130	°C
$h_{A,in}^2$	Secondary air relative humidity	0	g/kg
T_f	Furnace initial temperature	900	°C
$C_{SO_2}^0$	Furnace initial SO ₂ content	0	%
$C_{O_2}^0$	Furnace initial O ₂ content	21	%
$C_{N_2}^0$	Furnace initial N ₂ content	79	%

Figure 5 displays the dynamic behavior of the temperature due to the injection of 32 m³/h of the liquid sulfur at a temperature of 132 °C, in addition to 599 m³/h of the dry air at a temperature of 130 °C into the sulfur combustion furnace. It illustrates the dynamic

variation in the combustion gas temperature at the outlet of the sulfur combustion furnace and the temperature profile along the flow across the combustion chamber length. Length 0 indicates the entrance of the furnace, while length 1 indicates the exit.

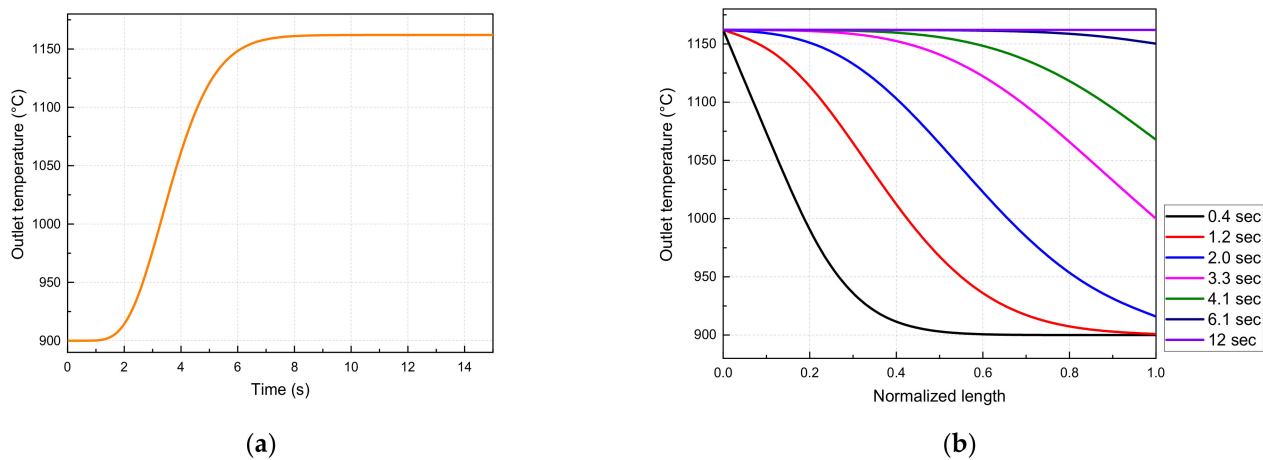


Figure 5. Dynamic response of the temperature: (a) temperature variation at the outlet of the combustion furnace; (b) temperature evolution across the combustion chamber.

According to the simulation results, it is shown that the temperature of the gas mixture at the outlet of the combustion furnace increases from 900 °C to 1162 °C, which represents the flame temperature value produced by the atomized sulfur oxidation. It is noticeable that the oxidation reaction occurs in the first layers of the combustion chamber length, which is reasonable due to the rapid kinetics of the tiny sulfur droplet oxidation. As time proceeds, the temperature of each layer in the combustion furnace starts increasing until reaching the maximal temperature. Within less than 12 s, the combustion furnace temperature reaches the steady state at a temperature of 1162 °C.

When it comes to the combustion gas mixture composition, Figure 6 illustrates the temporal variation in the SO₂ and the O₂ at the outlet of the combustion furnace and along the combustion chamber length. After the complete oxidation of the liquid sulfur in the first layer of the combustion chamber, a gas mixture consisting of 12%, 9%, and 79% of SO₂, O₂, and N₂, respectively, is produced. The combustion gas mixture flows through the combustion chamber, which initially contains 21% of O₂ and 79% of N₂. As shown in the simulation results, the molar fraction of SO₂ increases within the combustion chamber up to a value of 12%, while the molar fraction of O₂ decreases down to a value of 9%. After a transient time of 12 s, approximately, the gas mixture at the outlet of the combustion furnace reaches a steady state composition of 12%, 9%, and 79% of SO₂, O₂, and N₂, respectively. Note that the inert gas, N₂, is not involved in the oxidation reaction and only flows from the entrance to the exit of the combustion chamber.

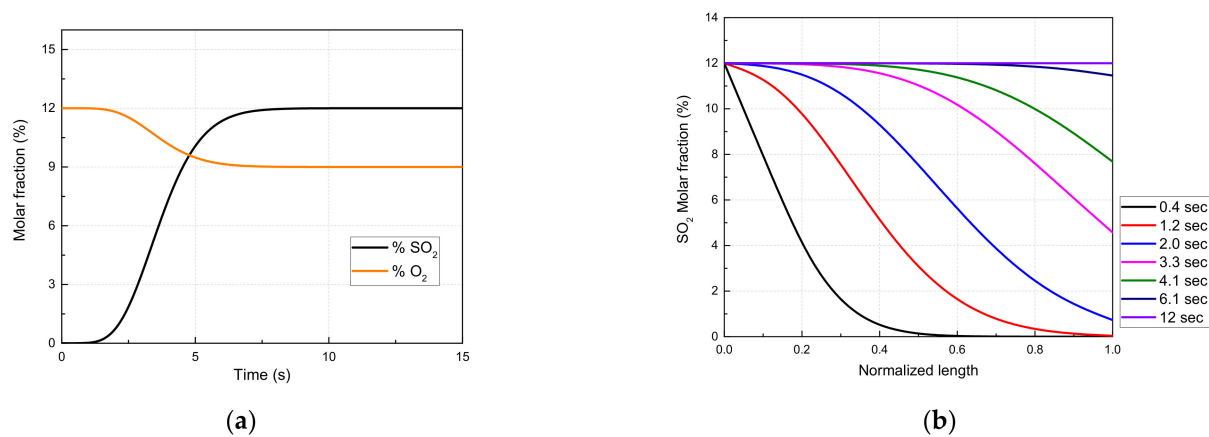


Figure 6. Dynamic response of the SO_2 molar fraction: (a) variation in the SO_2 molar fraction at the outlet of the combustion furnace; (b) SO_2 molar fraction evolution across the combustion chamber.

5. Model Validation

To evaluate the performance of the proposed model, data from the studied industrial unit were generated using the plant PI System. The collected data include the temporal variation in the sulfur combustion furnace inlet parameters, knowing the liquid sulfur flow rate $\dot{Q}_{S,\text{in}}$ and temperature $T_{S,\text{in}}$, the primary and secondary combustion air supply flowrates $\dot{Q}_{A,\text{in}}^1$ and $\dot{Q}_{A,\text{in}}^2$, temperatures $T_{A,\text{in}}^1$ and $T_{A,\text{in}}^2$, and air humidity values $h_{A,\text{in}}^1$ and $h_{A,\text{in}}^2$. Thus, the humidity measurement was used to estimate the molar fractions $X_{\text{O}_2,\text{in}}^1$, $X_{\text{N}_2,\text{in}}^1$, $X_{\text{O}_2,\text{in}}^2$, and $X_{\text{N}_2,\text{in}}^2$. For the sulfur combustion furnace outlet parameters, the gas mixture temperature T_{out} at the outlet was collected.

Firstly, the proposed model was tested using the plant data in a period of 60 min, with a sampling time of 1 s, by updating the inlet parameters of the model and reading back the simulation results. Secondly, the model was run in a period of 300 h with a sampling time of 1 min, which corresponds to a period of 12.5 days. Afterwards, obtained temperature values of the gas mixture at the outlet of the furnace were compared with industrial measurement. The testing period was chosen so that different operating conditions of the process could be covered, extracted, and then tested using the proposed model. The liquid sulfur flow rate encountered variations between $20 \text{ m}^3/\text{h}$ and $33 \text{ m}^3/\text{h}$, while the combustion air supply took values between $300 \text{ m}^3/\text{h}$ and $600 \text{ m}^3/\text{h}$. When it comes to the air and the liquid sulfur temperatures, the corresponding value changed slightly around $128 \text{ }^\circ\text{C}$ and $132 \text{ }^\circ\text{C}$, respectively.

Figure 7 illustrates the dynamic response of the studied system and the developed model under variations in the liquid sulfur and the combustion air flow rates. Firstly, the liquid sulfur flow rate varied slightly from $25.2 \text{ m}^3/\text{h}$ to $25.6 \text{ m}^3/\text{h}$ while keeping the first air flow rate constant at a value of $445 \text{ m}^3/\text{h}$. As shown in the simulation results, the temperature of the gas mixture at the outlet of the combustion furnace increased from $950 \text{ }^\circ\text{C}$ to $968 \text{ }^\circ\text{C}$. This temperature increase is justified by the exothermicity of the combustion liquid reaction that generates heat proportionally to the liquid sulfur flow rate. By increasing both the liquid sulfur flow rate and the first air flow rate to a value of 27.6 m^3 and $565 \text{ m}^3/\text{h}$, respectively, it is observed that the temperature at the sulfur furnace outlet increases up to $985 \text{ }^\circ\text{C}$ and decreases thereafter down to $956 \text{ }^\circ\text{C}$. In the face of flow rate changes at the inlet of the sulfur combustion furnace, it is well recognized that the simulated temperature follows the plant measurement with an acceptable accuracy.

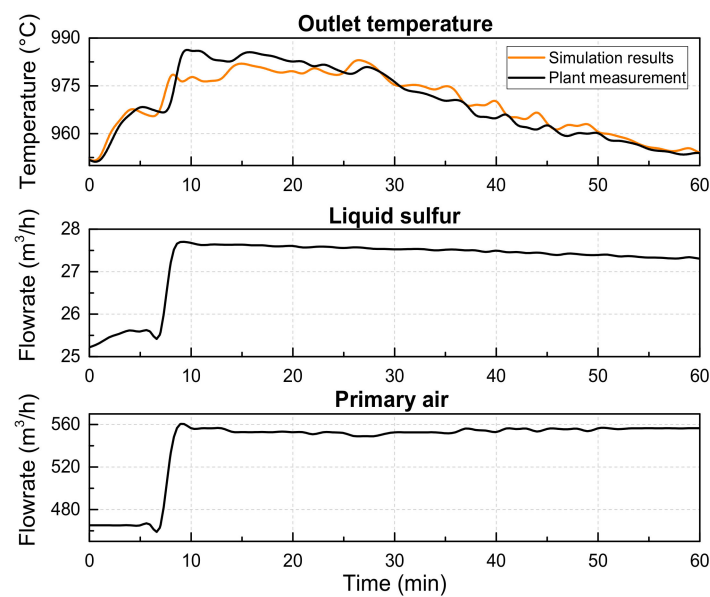


Figure 7. Comparison of the sulfur combustion furnace predicted and measured outlet temperature in response to inlet flow rate changes.

Moreover, Figure 8 shows the predicted outlet temperature variations compared to the plant-measured value at the outlet of the sulfur combustion furnace in a period of 12.5 days. It is noticed that the proposed model is able to quite closely predict and track the observed variations in the measured temperature values at different operating conditions.

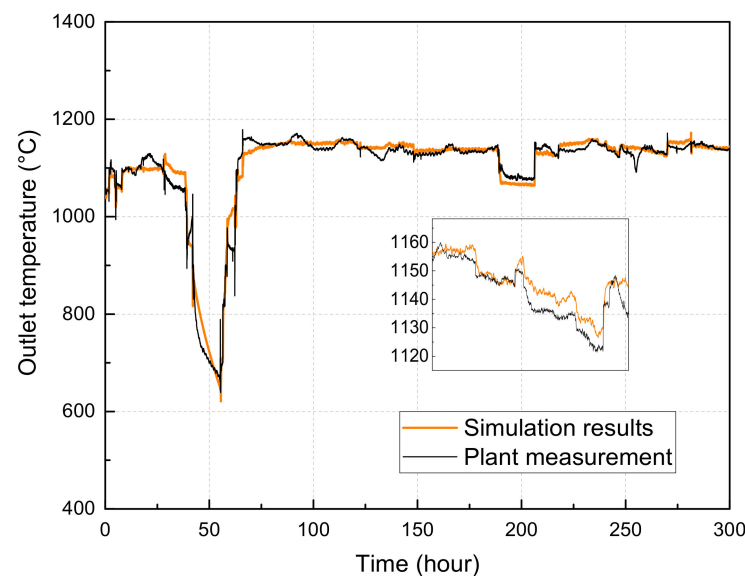


Figure 8. Measured and predicted temperature value at the outlet of the combustion furnace.

To determine the model efficiency and quality, real plant data are used and compared to the model-predicted values. In this study, three statistical coefficients were used, knowing the determination coefficient R^2 , the mean absolute error MAE, and the root mean square error RMSE. The formula used to calculate each coefficient is given by:

$$R^2 = 1 - \frac{\sum_{j=1}^N (T_m^j - T_p^j)}{\sum_{j=1}^N (T_m^j - \bar{T}_m)} \quad (42)$$

$$\text{MAE} = \frac{\sum_{j=1}^N (T_m^j - T_p^j)}{N} \quad (43)$$

$$\text{RMSE} = \sqrt{\frac{\sum_{j=1}^N (T_m^j - T_p^j)^2}{N}} \quad (44)$$

where:

- T_m^j : measured outlet temperature ($^{\circ}\text{C}$);
- T_p^j : predicted outlet temperature ($^{\circ}\text{C}$);
- N : measurement number.

According to the simulation results and plant measurements, the proposed model showed high accuracy in predicting the outlet temperature of the studied sulfur combustion furnace with a determination coefficient of $R^2 = 0.96$, a mean absolute error of $\text{MAE} = 16.12$ $^{\circ}\text{C}$, and a root mean square error of $\text{RMSE} = 23.27$ $^{\circ}\text{C}$.

6. Parametric Study

To better understand the effect and the relationship between the sulfur combustion furnace inlets and outlets, a parametric study was conducted in steady state using the validated proposed model. As seen in the model validation part, several parameters affect the sulfur combustion furnace outlet. In sulfur acid manufacturing plants, the sulfur is primarily filtered and melted before being transported to the combustion furnace. It is kept in the molten phase using steam jackets and pipes. Thus, the temperature of liquid sulfur at the inlet to the furnace may change during the transportation pumping phase. Note that liquid sulfur flow rate at the combustion furnace is adjusted based on the plant production rate. When it comes to the combustion air, it is first dried before being used in the combustion furnace using air blowers. However, the temperature and the humidity of the combustion air can fluctuate because of the drying and the blowing process performance.

In this parametric study, the inputs and outputs of the sulfur combustion furnace were classified as follows: the manipulated inputs are the liquid sulfur flow rate and the combustion air flow rate; the disturbance inputs are the liquid sulfur temperature and the combustion air temperature; the outputs are the furnace outlet temperature and the combustion gas composition (SO_2 , O_2 and N_2).

6.1. Effect of the Liquid Sulfur and the Combustion Air Flow Rates on the Gas Composition

To study the effect of the liquid sulfur flow rate and the combustion air flow rate, the two corresponding values were varied and converted into the term of the air/sulfur flow rates ratio. Figure 9 illustrates the air/sulfur flow rate ratio variation on the gas mixture composition at the outlet of the combustion furnace. In this manipulation, several values ranging between 0 and 30 of the air/sulfur flow rates ratios were tested. Based on the simulation results, it is shown that the increase in the air/sulfur flow rates ratio at the inlet of the combustion furnace increases the SO_2 molar fraction and decreases the oxygen molar fraction at the outlet until the complete oxidation of the atomized sulfur. Note that the air/sulfur flow rates ratio of 8.96:1 (=4.76 mol of air/mol sulfur) corresponds to the stoichiometric combustion ratio necessary for a complete consumption of both the sulfur and the oxygen, without an excess left over. From the stoichiometry of the sulfur oxidation reaction, it is obvious that the oxidation of 1 mol of the atomized sulfur requires 1 mol of oxygen and $\frac{79}{21} \times 1 = 3.76$ mol of nitrogen, which is equal to the stoichiometric combustion ratio of the sulfur oxidation.

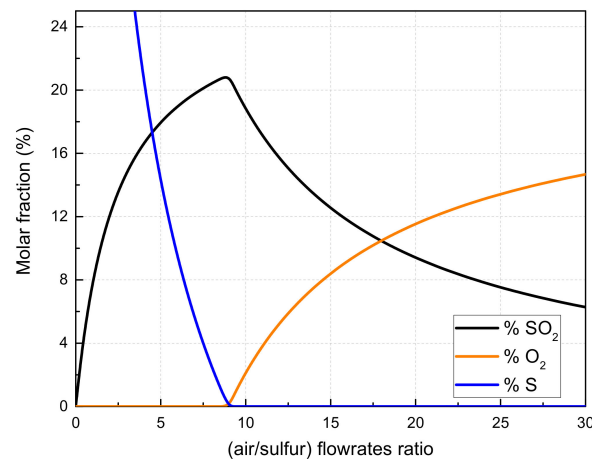


Figure 9. Effect of excess air on the combustion gas composition.

In Figure 9, the SO₂ molar fraction increases up to 21%, which represents the initial O₂ molar fraction contained in the combustion air. Above the stoichiometric combustion ratio, the air/sulfur ratio decreases the SO₂ molar fraction and increases the oxygen molar fraction. To achieve a chemical composition of 12%, 9%, and 79%, which is the optimum composition for the SO₂ catalytic conversion, it is necessary to operate with an air/sulfur flow rate ratio around 15.6:1.

6.2. Effect of the Liquid Sulfur and the Combustion Air Flow Rates on the Outlet Temperature

Regarding the temperature at the outlet of the sulfur combustion furnace, Figure 10 shows the effect of the air/sulfur flow rates ratio on the combustion gas temperature. In this manipulation, the air/sulfur flow rates ratio was varied from 13:1 to 20:1, while the blown air and the liquid sulfur temperatures were set to 130 °C and 132 °C, respectively. It reveals that the temperature at the furnace outlet decreases by raising the air/sulfur flow rates ratio at the furnace inlet. Thus, increasing the air/sulfur flow rates ratio by one point may dramatically decrease the temperature of the combustion gas mixture. The obtained result is because a part of the heat generated by the sulfur oxidation is absorbed by the excess air contained in the combustion gas. In contrast, increasing the liquid sulfur flow rate at the furnace inlet increases the temperature of the gas mixture at the outlet. This result is reasonable since the chemical reaction governing the combustion furnace is a highly exothermic reaction that generates heat proportionally to the consumed sulfur. The average of the heat produced by the oxidation of 1 mole of the liquid sulfur is about 298,190 kJ.

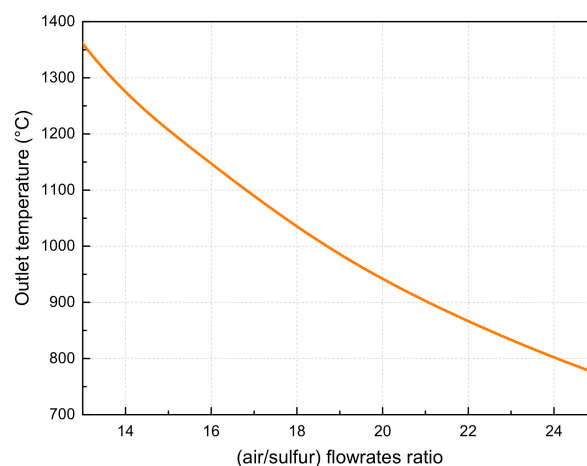


Figure 10. Effect of excess air on the combustion gas temperature.

6.3. Effect of the Blown Air Temperature on the Outlet Temperature

As shown in Figure 11, it is important to mention that the temperature of the blown air has an impact on the temperature of the combustion gas at the furnace outlet. At an air/sulfur flow rates ratio of 15.6:1, the temperature of the combustion gas at the outlet achieves 1143 °C, 1167 °C, and 1183 °C while operating with the blown air at the temperature of 100 °C, 130 °C, and 150 °C, respectively. Thus, operating with the same air/sulfur flow rates ratio value, the temperature of the combustion gas at the furnace outlet increases as the blown air temperature increases at the furnace inlet. This is because the blown air heat increases by raising its temperature, which provides more heat to the gas mixture within the combustion furnace. Through the simulations carried out, it is shown that temperature of the liquid sulfur does have a relevant impact on the outlet temperature. Thus, the outlet temperature is impacted by both the air/sulfur flow rates ratio and the blown air inlet temperature.

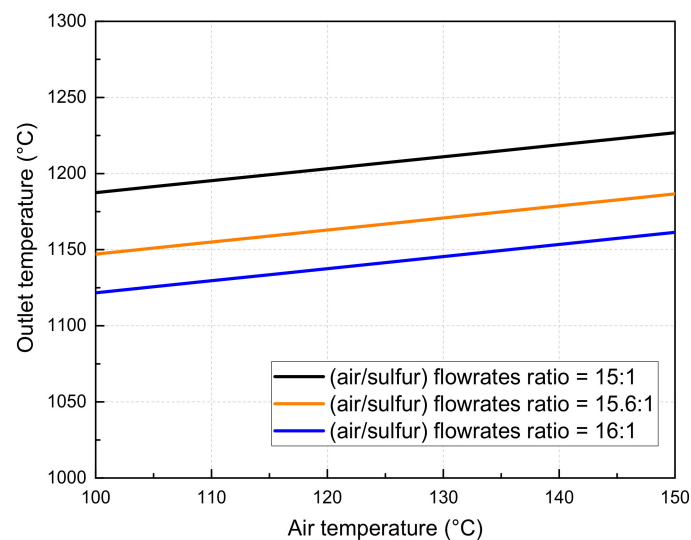


Figure 11. Effect of blown air temperature on the combustion gas temperature.

6.4. Relationship between the Furnace Outlet Temperature and the SO₂ Molar Fraction

Based on the parametric study results, four conclusions may be drawn. Increasing air/liquid sulfur flow rates ratio at the inlet of the sulfur combustion furnace: (1) reduces the SO₂ molar fraction, (2) raises the O₂ molar fraction, and (3) decreases the gas mixture temperature. Industrially, the gas mixture temperature and chemical composition are controlled based on the air/liquid sulfur flow rates ratio. However, the impact of the blown air temperature must also be considered during the control operation since it represents a disturbance input to the combustion sulfur furnace. Based on the proposed model, several simulations were conducted by varying the air/liquid sulfur flow rates ratio and the blown air temperature and tracking the variation in the gas mixture temperature and the SO₂ molar fraction at the furnace outlet.

Figure 12 illustrates the relationships between the temperature and the SO₂ molar fraction at the outlet of the furnace at different blown air temperature values, ranging between 100 °C and 150°. It is shown that a rise in the temperature at the outlet of the sulfur combustion burner reflects an improvement in the SO₂ molar fraction present in the gas combustion gas at different blown air temperatures. As well, the chemical composition at the outlet of the sulfur combustion furnace can be perfectly estimated based on the measurement of the outlet temperature and the blown air temperature.

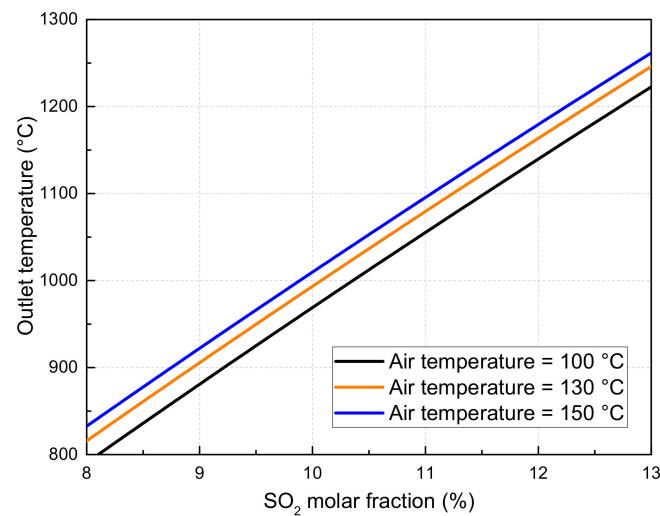


Figure 12. Relationship between the furnace outlet temperature and the SO₂ molar fraction.

In a sulfuric acid manufacturing plant, temperature sensors are extensively used at different stages to monitor the plant operation and performance. They are employed to measure the temperature of the blown air, the liquid sulfur, the outlet of the sulfur combustion furnace, the inlet, and the outlet of each catalytic bed, in addition to the inlet and the outlet of the absorption towers. However, when it comes to the SO₂ concentration, sensors are generally missing and measurements are taken periodically in an offline way. Therefore, the development of a model for the SO₂ molar fraction measurement is of great interest.

Referring to the model development section and assuming complete oxidation of the atomized sulfur, the temperature and the chemical composition at the outlet of the sulfur combustion furnace can be expressed in steady state by:

$$\left\{ \begin{array}{l} \dot{F}_{O_2,out} = 0.21\dot{F}_{A,in} - \dot{F}_{S,in} \\ \dot{F}_{S,out} = 0 \\ \dot{F}_{SO_2,out} = \dot{F}_{S,in} \\ \dot{F}_{N_2,out} = 0.79\dot{F}_{A,in} \\ \dot{F}_{total,out} = \dot{F}_{A,in} \\ \int_{T_0}^{T_{out}} \sum_i \dot{F}_{i,out} c_{p,i}(T) \cdot dT = \int_{T_0}^{T_{in}} \sum_i \dot{F}_{i,out} c_{p,i}(T) \cdot dT + \dot{F}_{S,in} \cdot \Delta_r H \end{array} \right. \quad (45)$$

Applying an approximation to the specific heat capacity computation $c_{p,i}(T) \simeq c_{p,i}(T_0)$ leads to:

$$T_{out} = T_0 + \frac{(\dot{F}_{A,in} c_{p,Air} + \dot{F}_{SO_2,out} c_{p,S})(T_{in} - T_0) + \dot{F}_{SO_2,out} \Delta_r H}{\dot{F}_{A,in} c_{p,Air} + (c_{p,SO_2} - c_{p,O_2}) \dot{F}_{SO_2,out}} \quad (46)$$

The initial temperature T_{in} of the gas mixture before the oxidation reaction is given by:

$$T_{in} = T_0 + \frac{\dot{F}_{A,in} c_{p,Air} (T_{A,in} - T_0) + \dot{F}_{S,in} c_{p,S} (T_{S,in} - T_0)}{\dot{F}_{A,in} c_{p,Air} + \dot{F}_{S,in} c_{p,S}} \quad (47)$$

Substituting Equation (47) in (46):

$$T_{out} = T_0 + \frac{\dot{F}_{A,in} c_{p,Air} (T_{A,in} - T_0) + \dot{F}_{SO_2,out} c_{p,S} (T_{S,in} - T_0) + \dot{F}_{SO_2,out} \Delta_r H}{\dot{F}_{A,in} c_{p,Air} + (c_{p,SO_2} - c_{p,O_2}) \dot{F}_{SO_2,out}} \quad (48)$$

Hence, the SO₂ molar fraction $X_{\text{SO}_2,\text{out}}$ can be estimated based on the gas mixture measured temperature T_{out} at the outlet of the sulfur combustion furnace and the other measured temperatures ($T_{\text{A,in}}$, $T_{\text{S,in}}$) by the following approximated equation:

$$X_{\text{SO}_2,\text{out}} = \frac{c_{p,\text{Air}}(T_{\text{A,in}} - T_{\text{out}})}{(T_{\text{out}} - T_0)(c_{p,\text{SO}_2} - c_{p,\text{O}_2}) - \Delta_r H - c_{p,\text{S}}(T_{\text{S,in}} - T_0)} \quad (49)$$

As illustrated by Equation (49), the SO₂ molar fraction $X_{\text{SO}_2,\text{out}}$ is correlated with the furnace outlet temperature T_{out} at different blown air and liquid sulfur temperature values ($T_{\text{A,in}}$, $T_{\text{S,in}}$). Increasing the temperature of the blown air at the inlet of the furnace linearly increases the temperature and the SO₂ molar fraction at the furnace outlet. However, considering the fact that $\Delta_r H \gg c_{p,\text{S}}(T_{\text{S,in}} - T_0)$, the impact of the liquid sulfur temperature is generally neglected in this correlation. These results were encountered and mentioned during the simulations performed in the parametric study and they were extensively validated using industrial measurement.

7. Conclusions

In the present work, a study on sulfur combustion furnace modeling and simulation was investigated. The sulfur combustion furnace was modeled based on the fundamental mass and energy balance equations in steady state and dynamic mode. Compared to existing studies, the proposed model incorporates major process variables and considers the oxidation reaction aspect and the flow dynamic behavior in the furnace and it does not require any complex parameter estimation or calibration. The simulation of the proposed model was conducted in the Matlab/Simulink environment, using level 2 Matlab s-functions. To validate the model, data from the industrial sulfuric acid process were used. Comparing the model simulation results with the industrial measurement, an accuracy of 96% was found with an absolute error of 6.12 °C and a root mean square error of 23.27 °C.

Based on the developed model, several simulations were performed to study the effects the sulfur combustion furnace input variables on the output, knowing the impact of the excess air, the blown air temperature, and the liquid sulfur temperature. The parametric study is a necessary and helpful step that serves in understanding the relationship between the furnace key variables and optimizing the operation performance. Obtained results reveal that with an increase in excess air, the inlet decreases the temperature and the SO₂ molar fraction at the outlet of the sulfur combustion furnace. In addition, a rise in the blown air temperature improves the temperature of the combustion gas mixture, while the liquid sulfur temperature did not show a significant effect on the outlet. Through the parametric study, a high correlation between the SO₂ molar fraction and the combustion gas mixture temperature was noticed. Thus, the relationship between the temperature and the SO₂ molar fraction at the outlet of the sulfur combustion furnace was investigated to ensure an accurate estimation of the combustion gas mixture SO₂ content based on the process-measured variables.

The developed model can be used to predict and optimize the performance of the sulfur combustion furnace, which represents the basic stage in each sulfur acid plant. In this perspective, future work will be carried out to develop a digital twin for the sulfur combustion furnace based on the developed model.

Author Contributions: Conceptualization, A.M., A.S. and M.S.; methodology, A.M.; software, A.M.; validation, A.M. and A.B.; formal analysis, A.M. and A.B.; investigation, A.M. and A.B.; resources, A.M. and A.B.; data curation, A.B.; writing—original draft preparation, A.M. and R.O.; writing—review and editing, A.M. and R.O.; visualization, A.M.; supervision, A.S., M.S. and K.B.; project administration, H.G.; funding acquisition, H.G. All authors have read and agreed to the published version of the manuscript.

Funding: This research was funded by Innovation Lab for Operations of UM6P.

Data Availability Statement: The data used in this study were provided by OCP and ILO under Digitalization Projects.

Conflicts of Interest: The authors declare no conflict of interest.

References

1. Conroy, E.H.; Johnstone, H.F. Combustion of Sulfur in a Venturi Spray Burner. *Ind. Eng. Chem.* **1949**, *41*, 2741–2748. [[CrossRef](#)]
2. Sander, U.H.F.; Fischer, H.; Rothe, U.; Kola, R. *Sulphur, Sulphur Dioxide and Sulphuric Acid*; British Sulphur Corporation: London, UK, 1984.
3. Moeller, W.; Winkler, K. Control, and undefined 1968. In *The Double Contact Process for Sulphuric Acid Production*; Taylor & Francis: Abingdon, UK, 1968; Volume 18, pp. 324–325. [[CrossRef](#)]
4. Louie, D.K. *Handbook of Sulphuric Acid Manufacturing*; DKL Engineering, Inc.: Aurora, ON, Canada, 2005.
5. Kiss, A.A.; Bildea, C.S.; Grievink, J. Dynamic modeling and process optimization of an industrial sulfuric acid plant. *Chem. Eng. J.* **2010**, *158*, 241–249. [[CrossRef](#)]
6. Zhang, F.; Heidarifatasm, H.; Harth, S.; Zirwes, T.; Wang, R.; Fedoryk, M.; Sebbar, N.; Habisreuther, P.; Trimis, D.; Bockhorna, H. Numerical evaluation of a novel double-concentric swirl burner for sulfur combustion. *Renew. Sustain. Energy Rev.* **2020**, *133*, 110257. [[CrossRef](#)]
7. Rangaiah, G.P.; Sharma, S.; Lin, H.W. Evaluation of two termination criteria in evolutionary algorithms for multi-objective optimization of complex chemical processes. *Chem. Eng. Res. Design* **2017**, *124*, 58–65. [[CrossRef](#)]
8. Teh, S.Y.; Chua, K.B.; Hong, B.H.; Ling, A.J.W.; Andiappan, V.; Foo, D.C.Y.; Hassim, M.H.; Ng, D.K.S. A Hybrid Multi-Objective Optimization Framework for Preliminary Process Design Based on Health, Safety and Environmental Impact. *Processes* **2019**, *7*, 200. [[CrossRef](#)]
9. Farooq, M.; Muñoz, D.A.; Chowdhury, N.B.; Hasan, Z.; Biplob, A.H.M. HYSYS simulation of a sulfuric acid plant and optimization approach of annual profit. *J. Sci.* **2012**, *2*, 179–182.
10. Sultana, S.T.; Amin, M.R. Aspen-Hysys Simulation Of Sulfuric Acid Plant. *J. Chem. Eng.* **2012**, *26*, 47–49. [[CrossRef](#)]
11. Tejada-Iglesias, M.; Szuba, J.; Koniuch, R.; Ricardez-Sandoval, L. Optimization and Modeling of an Industrial-Scale Sulfuric Acid Plant under Uncertainty. *Ind. Eng. Chem. Res.* **2018**, *57*, 8253–8266. [[CrossRef](#)]
12. Nouri, H.; Ouederni, A. Experimental and modeling study of sulfur dioxide oxidation in packed-bed tubular reactor. *Int. J. Innov. Appl. Stud.* **2013**, *3*, 1045–1052.
13. Sørensen, P.A.; Møllerhøj, M.; Christensen, K.A. New dynamic models for simulation of industrial SO₂ oxidation reactors and wet gas sulfuric acid plants. *Chem. Eng. J.* **2015**, *278*, 421–429. [[CrossRef](#)]
14. He, J.; Zhang, J.; Shang, H. Dynamic modelling and simulation of the sulphur dioxide converter in an industrial smelter. *Can. J. Chem. Eng.* **2019**, *97*, 1838–1847. [[CrossRef](#)]
15. Mounaam, A.; Oulhiq, R.; Souissi, A.; Salouhi, M.; Benjelloun, K.; Bichri, A. A Model-Driven Digital Twin Framework Development for Sulfur Dioxide Conversion Units Simulation. *Adv. Sci. Technol. Eng. Syst. J.* **2021**, *6*, 122–131. [[CrossRef](#)]
16. Zaker, M.R.; Fauteux-Lefebvre, C.; Thibault, J.; Annesini, C.; Murmura, M.A. Modelling and Multi-Objective Optimization of the Sulphur Dioxide Oxidation Process. *Processes* **2021**, *9*, 1072. [[CrossRef](#)]
17. Mounaam, A.; Oulhiq, R.; Souissi, A.; Salouhi, M.; Benjelloun, K. Dynamic Modeling, Simulation and Study of a Sulfur Burning Unit in an Industrial Sulfuric Acid Plant. In Proceedings of the 18th IEEE International Multi-Conference on Systems, Signals and Devices, SSD 2021, Monastir, Tunisia, 22–25 March 2021; pp. 921–926. [[CrossRef](#)]
18. Mounaam, A.; Harmen, Y.; Chhiti, Y.; Souissi, A.; Salouhi, M.; el Khouakhi, M. UniSim-design simulation and analysis of a sulphuric acid manufacturing plant with double absorption process. In Proceedings of the SIMULTECH 2020—Proceedings of the 10th International Conference on Simulation and Modeling Methodologies, Technologies and Applications, Online, 8–10 July 2020; pp. 91–100. [[CrossRef](#)]
19. King, M.; Moats, M.; Davenport, W. *Sulfuric Acid Manufacture: Analysis, Control and Optimization*; Elsevier: Amsterdam, The Netherlands, 2013.
20. Tobolsky, A.V.; Eisenberg, A. Equilibrium Polymerization of Sulfur. *J. Am. Chem. Soc.* **1959**, *81*, 780–782. [[CrossRef](#)]
21. Froment, G.; Bischoff, K.; de Wilde, J. *Chemical Reactor Analysis and Design*; Wiley: Hoboken, NJ, USA, 1990.
22. Bird, R.B.; Stewart, W.E.; Lightfoot, E.N. *Fenòmenos de Transporte*; John Wiley & Sons, Inc.: Hoboken, NJ, USA, 2016; Volume 1.
23. Brogioli, D.; Vailati, A. Diffusive mass transfer by nonequilibrium fluctuations: Fick's law revisited. *Phys. Rev. E Stat. Nonlin Soft Matter Phys.* **2001**, *63*, 0121051–0121054. [[CrossRef](#)] [[PubMed](#)]
24. Spencer, H.M. Empirical Heat Capacity Equations of Various Gases. *J. Am. Chem. Soc.* **1945**, *67*, 1859–1860. [[CrossRef](#)]
25. Mounaam, A.; Harmen, Y.; Chhiti, Y.; Souissi, A.; Salouhi, M.; Benjelloun, K.; Elkhouchi, M.; Deshayes, L. Dynamic behavior analysis of tubular heat exchanger: Experimental and theoretical study. In Proceedings of the 5th International Conference on Renewable Energies for Developing Countries (REDEC), Marrakech, Morocco, 29–30 June 2020; pp. 1–6.
26. Chakravarty, S. *Technology and Engineering Applications of Simulink*; IntechOpen Limited: London, UK, 2012.
27. Du, W. *Informatics and Management Science IV*; Springer: Berlin/Heidelberg, Germany, 2013.